Available online at www.sciencedirect.com

ScienceDirect

Procedia Structural Integrity 5 (2017) 973–980

Structural Integrity Procedia

www.elsevier.com/locate/procedia

2nd International Conference on Structural Integrity, ICSI 2017, 4-7 September 2017, Funchal, Madeira, Portugal

Development of a 2D analytical model for the prediction of directivity pattern of transducers in the generation of guided wave modes

Kumar Anubhav Tiwari[a,]*, Renaldas Raisutis[a] , Liudas Mazeika[a], Vykintas Samaitis[a]

[a]*Ultrasound Research Institute, Kaunas University of Technology, K. Barsausko st. 59 - A426, Kaunas LT-51423, Lithuania*

Abstract

The guided waves (GW) are extensively used in the nondestructive testing (NDT) and structure health monitoring (SHM) of the large and complex structures. It enables to detect the defects up to few meters away from the transducers. However, the defects could occur at longer distances. In order to cover the test area of interest for the estimation of defects and to find the exact position of the transducers to be glued/ embedded, the directivity pattern of the transducers must be known. The aim of the presented work is to develop the 2D analytical model for the estimation of directivity patterns of the transducers at various frequencies and distances. The model was developed using the Huygens's principle of wave propagation distances with considering the known phase dispersive characteristics of the guided wave modes in the medium. The principle of modelling will work to plot the directivity pattern at any distance, at any excitation frequency and with any configuration and shape of the transducers. In order to demonstrate the model, the directivity patterns of P1-type macro-fiber composite (MFC) transducer in the generation of fundamental Lamb modes and shear horizontal mode at 300 mm from the center of MFC were obtained. The input signal used was 80 kHz, 3 period signal and propagation medium was Al plate of 2 mm thickness. The prediction about the position of where MFC transducer should be placed or glued on the object and selection of proper wave modes in order to estimate the defects in various materials is also discussed. The results were validated using finite element analysis (FEA) performed in *ANSYS* and further verified by the experimental analysis using low-frequency (LF) ultrasonic measurement system *ULTRALAB,* developed by Ultrasound Research Institute, Kaunas University of Technology. The proposed analytical model will not only facilitate to decide the position and number of transducers but also leads to choosing the configuration of transducer and wave modes suitable to be used for the inspection of defects.

Peer-review under responsibility of the Scientific Committee of ICSI 2017

Keywords: Analytical model; Directivity; Macro fiber Composite (MFC); Lamb mode; Shear horizontal; Ultrasonic NDT; Transducer

* Corresponding author. Tel.: +370-64694913; fax: +370-37451489.
E-mail address: k.tiwari@ktu.lt

Peer-review under responsibility of the Scientific Committee of ICSI 2017
10.1016/j.prostr.2017.07.139

1. Introduction

Structural health monitoring (SHM) systems are used to improve the safety, reliability and tracking of various complex structures, by combining the arrays of transducers in order to capture the required data. There are many techniques developed to implement the SHM systems. For example, Giurgiutiu (2005) uses the electro-mechanical (E/M) impedance method for detecting the damages in thin plates and aerospace structures and Zagrai and Cakan (2010) tested the structural damages in simple and complex metallic structures using the Magneto-mechanical impedance (MMI) method. Another efficient SHM system was proposed by Katsikeros and Labeas (2009) which was based on strain measurements and its processing was performed by Artificial Neural Network (ANN). The review of acoustic emission techniques for health monitoring of bridge structures was performed by Nair and Cai (2010). The various SHM systems utilizing the guided waves (GW) for the inspection of defects and delaminations were discussed by Raghavan and Cesnik (2007) which was reviewed again by Mitra and Gopalakrishnan (2016). Out of these methods, GW testing to estimate the size, location and type of defects is one of the most suitable techniques in the field of non-destructive testing (NDT) and SHM applications. This method of testing is based on the excitation and reception of the ultrasonic GW. It requires the actuators and sensors to be embedded/ glued on the structure to cover the region of interest. The receiving transducers can be a contact or non-contact types as described by Tiwari and Raisutis (2016) which can be chosen depending on the requirements. In spite of the merits associated with GW testing of structures, there are some complications related to the analysis of captured signals. Due to the mode conversion, multiple reflections and variation of wave parameters with environmental conditions, the signal processing becomes quite difficult.

GW testing is very handy for the inspection of defects up to few meters away from the transmitter. However, the defects could occur at longer distances. The long range testing using guided waves were demonstrated by Wilcox (2000), Guo and Kundu (2001), Alleyne et al. (2004), Loveday and Long (2014) and Zhang, Han and Yuan (2013). Due to the large propagation distance, GW is required to rapidly inspect the structure from the fixed position of transmitting transducer or using the array of transducers. That is why directivity pattern of the transducer is an important parameter to be evaluated parameter to be known for the effective setup of the SHM systems. The directivity patterns depict about the coverage area and wave intensity in order to decide the excitation frequency and position of the transducers on the object to be tested. In addition, it also facilitates to decide the optimum number of transducers required for testing or monitoring the whole structure which in turn reduces the overall cost of the entire system. The objective of this work was to develop the 2D analytical model for the estimation of directivity patterns of the transducers at various frequencies and distances.

The presented work proposes a 2D analytical model based on Huygens's principle of wave propagation distances for the calculation of directivity patterns of the transducers for the generation of guided waves. The macro fiber transducer (MFC) of type P1 manufactured by Smart Material Smart-material.com (2017) was analysed for the development of the analytical model. It was investigated by Wilkie et al. (2000) and Ren and Jhang (2013) that MFC transducer could effectively generate and detect the Lamb waves for the estimation of defects in materials. Section 2 gives an introduction to directive characteristics of transducers and its dependency on influencing factors. The development of the analytical model is discussed in section 3. The results obtained from the analytical model are expressed in Section 4 which is also validated by finite element analysis (FEA) and experimental analysis. Finally, the conclusion and summary of this research work have been highlighted in section 5.

2. Directivity pattern of the transducer

Many theoretical and practical prospects to analyze the directivity pattern of the transducers have been developed. The transducer behavior in both time and the spatial domain is a key aspect for the accurate measurements. Ploss, Rupitsch and Lerch (2014) explained how the wrong assumptions lead to the incorrect measurement results. Directivity pattern of a transducer is a function of spatial angle (aperture), which depends on other factors such as the excitation frequency of operation and the size, shape and phase velocity dispersive characteristics of the wave propagation medium. Although, the directivity function is essentially a far field concept but it is not calculated at longer distances due to practical limitations.

Transducers are designed to have specific directivity patterns in a medium. The beam width of the directivity pattern is a function of the ratio of the diameter of the transducer to the wavelength of ultrasound waves. As the diameter of the transducer increases more as compared to the wavelength of ultrasound waves, beam width reduces accordingly. The main lobe of the directivity patterns contains most of the wave energy. There may be some side lobes as well in the pattern which occurs due to radiation in undesired directions, reflections etc. Transducers generally possess the same directivity patterns either they are operated as a transmitter or a receiver.

Many analytical and experimental methods have been developed in order to predict the directivity pattern of the transducers. The experimental analysis to plot the directivity patterns of circular shaped ultrasonic transducers was successfully performed by Umchid (2009). The mathematical expression to calculate the normalized directivity pattern of circular piston transducer is given by Kinsler et al. (2000):

$$H(\theta) = \left| \frac{2 J_1(ka \sin\theta)}{ka \sin\theta} \right| \tag{1}$$

Where J_1 is the first order Bessel function, a is the radius of the transducer and k is the wavenumber. Wavenumber k is expressed by $k = \frac{2\pi}{\lambda}$, λ is the wavelength.

Wenkang and Wenwu (2000) developed the model using FEA and successfully simulated the directivity pattern of the 1D transducer array. It was also found that the transducer size and material imposes a significant impact on the directivity pattern. The broadband directivity function can be expressed as a modulus of the complex directivity spectrum. This is verified by Leeman et al. (2001) who suggested the method for measuring the directivity function by locating the hydrophone at any distance from the transducer. The fast calculation to achieve the four-dimensional directivity pattern was successfully presented by Voelz (2012) for the phased array transducers. In this method, particle displacement field was represented by the dynamic Green's functions which transformed to the directivity patterns after normalizing the time axis. Li and Chan (2013) explained how directivity pattern of transducer arrays depends on the mutual radiation impedance between the elements and appropriate modifications must be performed in order to obtain the directivity function.

All these models need to have consideration about certain parameters and are limited to the specific applications, specific shape and configuration of transducers, type of propagation medium and excitation frequencies etc. There was a need of more versatile and simplified analytical model that could predict the directivity pattern of GW transducers possessing regular and arbitrary shape.

3. 2D Analytical model

The 2D analytical model has been developed using Huygens's principle of distances to plot the directivity pattern of GW of a transducer in any medium of known configuration and dispersive characteristics. Huygens's principle was originally proposed by C. Huygens, explained by Jenkins et al. (2014) and further described by Anon (2016). It states that all points on a wavefront are sources of wavelets which move and spread forward with the same velocity. The methodology of modelling is to considering the volume of transmitting zone as a series of points and calculating the magnitude and phase of distance vectors of each point source to the arbitrary receiving elements. After calculating and integrating the distance vectors between point sources to all receiving points, the B-scans of different modes are generated along the receiving zone. The other factors such as diffraction due to distances, correction factor considering the behaviour of the transducer and medium attenuation are also considered. The directivity patterns are then plotted by calculating the normalized peak-to-peak amplitudes of the signal components (*A-scans*) versus the angular position (polar coordinate system) of the propagating wave modes. It must be noted that the analytical model based on this principle will work for any configuration and shape of transducers providing that the dispersive characteristics of the medium and operating performance of the transducer are known.

The macro fiber composite (MFC-P1-2814) transducer (28 x 14mm) is used to describe the steps of modelling. The receiving zone in the medium/object was created by making an arc of radius R from the centre of MFC. The arc has been divided into k points (k=1, 2.....K) to plot the directivity pattern along the angles [(k-1) $\cdot\Delta_\alpha$], Δ_α is the increment

in angle, as shown in Fig. (1).

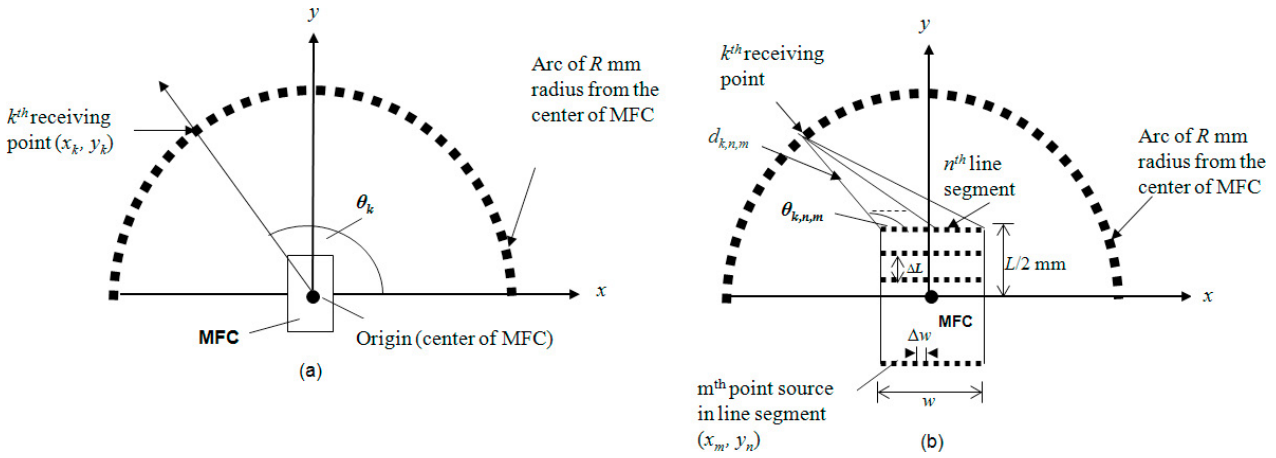

Fig. 1. Explanation of analytical modelling to find the directivity pattern of MFC at distance R: showing the origin at centre of MFC transducer and k^{th} receiving point (a), showing line segments, coordinates of m^{th} point source, distance vectors $d_{k,n,m}$ from all point sources to the sensing point and their angles $\theta_{k,n,m}$ (b), w and H are the width and height of the transducer (MFC) respectively.(w=14mm, H=28 mm for the MFC-P1 transducer)

If θ_k is the angle between the line joining the origin (centre of MFC) and k^{th} receiving/sensing point from the positive x-axis as shown in Fig. 1(a), the coordinates of the k^{th} point will be given as:

$$x_k = R \cdot \cos(\theta_k), y_k = R \cdot \sin(\theta_k) \tag{2}$$

The rectangular section has been created to represent the contour of MFC-P1-2814 or transmitting zone. The 2D coordinate system has been used containing the origin at the center of MFC. The length (L) and width (w) of MFC are directed along the y-axis and x-axis respectively. The MFC has been divided into n line segments (n=1, 2.....N) along the length with the step size of ΔL. Each line segment further divided into the m points (m=1, 2.....M) along the width with Δw separation distance which will act as individual point sources as shown in Fig. 1(b). Hence the coordinate of point sources will be (x_m ,y_n).

$$x_m = (m-1) \cdot \Delta w - w/2, y_n = (n-1) \cdot \Delta L - L/2 \tag{3}$$

The distance vector ($d_{k,n,m}$) from the m^{th} point on n^{th} line segment to the k^{th} sensing point and its corresponding angle ($\theta_{k,n,m}$) is expressed as follows:

$$d_{k,n,m} = \sqrt{(x_k - x_m)^2 + (y_k - y_n)^2} \tag{4}$$

$$\theta_{k,n,m} = \tan^{-1}\left[\frac{y_k - y_n}{x_k - x_m}\right] \tag{5}$$

After calculating the resultant propagation distance ($d_{k,n,m}$), the transfer function $H_T(f,d_{k,n,m})$ considering the attenuation and phase components, can be calculated as follows:

$$H_T(f, d_{k,n,m}) = \underbrace{e^{-\alpha(f) \cdot d_{k,n,m}}}_{\text{Attenuation part}} \cdot \underbrace{e^{-j\left(\frac{2 \cdot \pi \cdot f \cdot d_{k,n,m}}{V_{ph}(f,h)}\right)}}_{\text{Phase part}} \tag{6}$$

where $\alpha\ (f)$ is the frequency depended attenuation coefficient that can be assumed to be close to *zero* for the isotropic and lossless medium, V_{Ph} is the phase velocity which is the function of frequency f and plate thickness h.

The excitation signal $u_E(t)$ is applied at the transmitting zone (*i.e.* MFC in our case of consideration) and must be multiplied by the correction factor C_F corresponding to the specific GW mode as explained in Fig. 2. The value of C_F depends on the behaviour of the transducer and it is the value of amplitude factor $A_F(y)$ in the desired direction. The MFC operates in elongation mode and particle velocities of its upper and lower half remain in opposite phase (Fig.2 (a), Fig.2 (b)).The amplitude factor $A_F(y)$ is the ratio of y-coordinate of the point sources (y_n) to the half-length $(L/2)$ of the MFC as explained in Fig. 2(c) and Fig. 2(d). In order to calculate the C_F for the particular mode, the component of A_F needs to be calculated in the direction of the wave propagation as shown in Fig. 2(e).

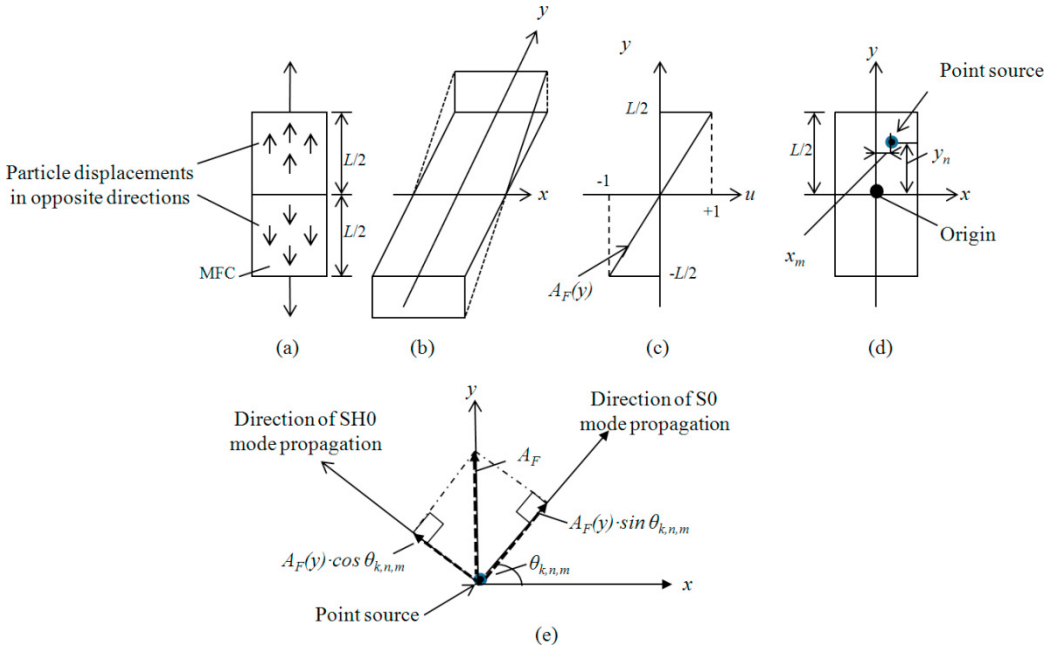

Fig.2. Calculation of correction factor (C_F) to be multiplied in excitation signal in case of MFC-P1: showing MFC-P1 operating in elongation mode (upper and lower half portion has opposite particle velocities) (a), 3D shape of MFC due to particle displacement (b), variations in the amplitude factor $A_F(y)$ with normalised particle velocity (u) (c) showing the coordinates of point source in order to calculate the $A_F(y)$ (d) and correction factor (C_F) (component of A_F in the direction of wave propagation) for the S0 mode ($A_F \cdot sin\ \theta_{L,P,I}$) and for the SH0 mode ($A_F \cdot cos\ \theta_{L,P,I}$) (e). The out-of-plane dominating component for the A0 mode is not shown for which C_F can be assumed to be 1.

In the case of MFC-P1, the value of C_F is $A_F \cdot \sin(\theta_{k,n,m})$, $A_F \cdot \cos(\theta_{k,n,m})$ for the S0 and SH0 mode respectively and C_F is 1 for the A0 mode as shown in Fig. 2(e).

Now, the spectrum of received signal at k^{th} receiving point will be expressed as follows:

$$U_{R,k}(f,\theta_k) = \sum_{n=1}^{N}\sum_{m=1}^{M} U_E(f)\cdot C_F . H_T(f,d_{k,n,m})\cdot \frac{1}{\sqrt{d_{k,n,m}}} \tag{7}$$

where $\frac{1}{\sqrt{d_{k,n,m}}}$ is the distance diffraction factor described in Morin (2010), $U_E(f)$ is the spectrum of the excitation signal $u_E(t)$ which is calculated by $FFT\ [u_E(t)]$, $U_{R,k}(f, \theta_k)$ is the spectrum of the received signal, θ_k is the angle in degree for the k^{th} receiving point.

The received signal in the time domain can be calculated by taking the inverse FFT.

$$u_{R,k}(t,\theta_k) = IFFT[U_{R,k}(f,\theta_k)] \tag{8}$$

The received signal $u_{R,k}(t, \theta_k)$ is the *A-scan* signal $A(t, \theta_k)$ at any k^{th} receiving point.

$$A(t,\theta_k) = u_R(t,\theta_k) \tag{9}$$

The peak-to-peak amplitude of the *A-scan* signals (A_{pp}) and the normalized peak-to-peak amplitude of the *A-scan* (A_{npp}) signal can be calculated as follows:

$$A_{pp}(\theta_k) = \max[A(t,\theta_k)] - \min[A(t,\theta_k)] \tag{10}$$

$$A_{npp}(\theta_k) = \left[\frac{A_{pp}(\theta_k)}{\max[A_{pp}(\theta_k)]}\right] \tag{11}$$

By varying the angle θ_k in polar coordinate system, $A_{npp}(\theta_k)$ can be evaluated and the directivity pattern in the polar coordinate system can be plotted.

4. Results

The directivity pattern of the S0, A0 and SH0 modes have been simulated by considering the aluminium plate having a thickness of 2 mm as a propagating medium. There are total 181(K=181) sensing points are assumed along the arc as shown in Fig 1. The length of MFC (L=28 mm) is divided into 15 (n=15) line segments with a step size of 1 mm (ΔL=1). Each line segment contains 15 point sources (m=15) with a step size of 1 mm (Δw=1). The 80 kHz, 3 periods excitation signal with a sampling frequency of 1.6 MHz and the Gaussian envelope was considered as an excitation signal. By varying the angle θ_1 from 0º to 180º, the directivity pattern of the received signal *in-plane* along the direction of propagation (the S0 mode), *in-plane* and perpendicular to the direction of propagation (the SH0) and *out-of-plane* (the A0) are generated at the distance of 300 mm (R=300). The directivity pattern in opposite direction along the lower half is just the mirror image of the upper half-circle. For simulation, the computational package Matlab (The *MathWorks*, Inc) was used. The complete directivity pattern from 0º to 360º is shown in Fig.3.

Fig 3(a) illustrates the strongly directional behaviour of the S0 mode. As shown in Fig. 3 (c), the width of the main lobe of the A0 mode is narrower (almost half) than the S0 mode. The directional behaviour of the A0 mode is also characterized by other minor lobes at the direction of 40º, 140º, 220º and 320º in addition to the main lobes at 90º and 180º. The SH0 mode is dominant along the direction of 40º, 140º, 220º and 320º and shown in Fig. 3(b). The reason behind these patterns can be explained as follows:

- MFC-P1 operates more effectively in elongation mode and that is why it possesses high directivity for the S0 mode which is dominant in the direction of wave propagation (along with the length of MFC).

- The wavelength (λ) at a frequency of 80 kHz is 67 mm for the S0 mode which is almost 2.5 times longer than the length of MFC (28 mm). On another hand, λ is just 14.83 mm for the A0 mode which is almost half of the length of MFC.

- The pattern of the SH0 is not along the normal to the direction of elongation (*i.e.* 0º and 180º) due to the behaviour of MFC-P1. As MFC-P1 operates in elongation (d33) mode, its upper and lower

half vibrates in opposite phases which produce forces to cancel out the pattern in 0º and 180º for the SH0 mode.

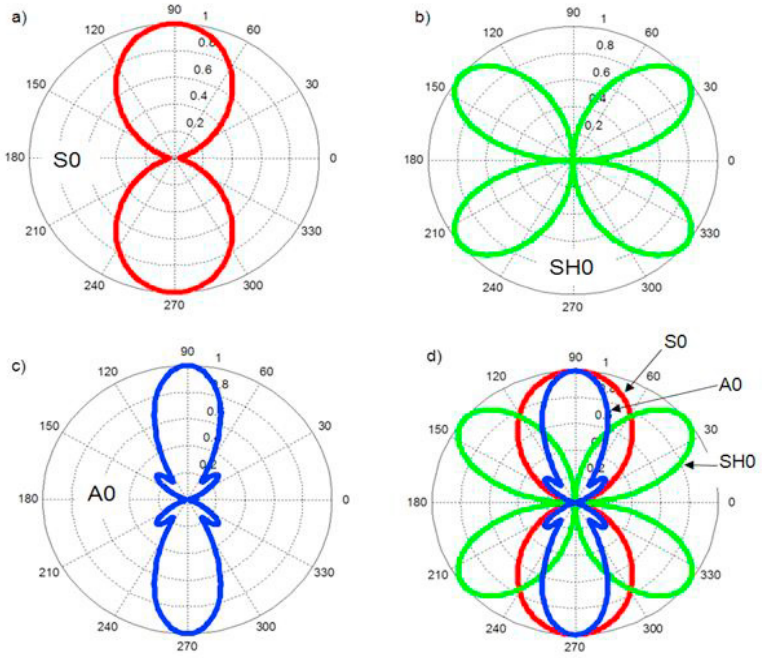

Fig. 3. Showing directivity patterns of the S0 mode (a), SH0 mode (b), A0 mode (c) and comparison of all three modes (d).

The results were also validated using FEA performed in *ANSYS* and further verified by the experimental analysis using the *ULTRALAB* low-frequency (LF) ultrasonic system (developed by the Ultrasound Research Institute of Kaunas University of Technology). The good agreement is achieved between the results obtained analytically and using FEA and experimental analysis.

5. Conclusions

The 2D analytic model was developed in order to predict the directivity pattern of the transducers in the case of generation of guided waves. The MFC-P1 transducer as a source and an aluminium plate as a propagation medium were used for the simulation. As the model is based on the integration of distances between the point sources and the sensing points, it is a universal 2D model which can be used to calculate the directivity pattern at any distance, excitation frequency with regular and arbitrary configuration and shape of the transducer. It should also be noted that by knowing the phase velocity dispersion of the wave propagating along the structure under investigation, the model will work for any propagation medium as well. It is observed from the resulting directivity patterns of MFC-P1 transducer that the A0 mode possessing the dominant *out-of-plane* component has a narrower pattern as compared to the S0 mode. This recommends increasing the number of MFC transducers for testing the larger area using the A0 modes. It was also observed that the shear horizontal (SH0) mode, instead of showing its directional behaviour along the perpendicular direction of propagation, is dominant at the directions of 45º, 135º, 225º and 315º. Therefore, the SH0 is not suitable to be used for the defect estimation in the direction of propagation.

The results were validated using FEA performed in *ANSYS* and further verified by the experimental analysis using the LF ultrasonic measurement system *ULTRALAB,* developed at the Ultrasound Research Institute of the Kaunas University of Technology. The experimental and simulation results obtained using FEA showed the good compromise with the analytical results. The proposed analytical model will not only facilitate to select the position and number of transducers but also leads to choosing the specific transducer and specific wave modes for the inspection of a particular type of defects.

Acknowledgements

This work was accomplished at the Ultrasound Research Institute, Kaunas University of technology, Lithuania.

References

Alleyne, D., Pavlakovic, B., Lowe, M. and Cawley, P., 2004. Rapid Long Range Inspection of Chemical Plant Pipework Using Guided Waves. Key Engineering Materials, 270-273, 434-441.

Anon, 2016. [Online] Available at: http://web.mit.edu/viz/EM/visualizations/coursenotes/modules/guide14.pdf [Accessed 13 Jan. 2016].

Giurgiutiu, V., 2005. Damage Detection in Thin Plates and Aerospace Structures with the Electro-Mechanical Impedance Method. Structural Health Monitoring, 4(2), 99–118.

Guo, D., Kundu, T., 2001. A new transducer holder mechanism for pipe inspection. The Journal of the Acoustical Society of America, 110(1), 303–309.

Jenkins, Francis A. and Watson, William W., 2014. Huygens' Principle. In AccessScience. McGraw-Hill Education.

Katsikeros, C.E. and Labeas, G.N., 2009. Development and validation of a strain-based Structural Health Monitoring system. Mechanical Systems and Signal Processing, 23(2), 372–383.

Kinsler, L. E., Frey ,A. R., Coppens , A. B., and Sanders , J. V., 2000. Fundamentals of Acoustics, Fourth Edition: John Wiley & Sons, Inc.

Leeman, S., Healey, A.J., Costa, E.T., Nicacio, H., Dantas, R.G. and Maia, J.M., 2001. Measurement of transducer directivity function. In Medical Imaging 2001, International Society for Optics and Photonics, 47-53.

Li, D. and Chen, H., 2013. Directivity calculation for acoustic transducer arrays with considering mutual radiation impedance. International Conference on Graphic and Image Processing (ICGIP 2012), 876864-876864.

Loveday, P.W. and Long, C.S., 2014. February. Long range guided wave defect monitoring in rail track. In D.E. Chimenti, L.J. Bond and D.O. Thompson eds., AIP Conference Proceedings , 1581 (1), 179-185.

Mitra, M. & Gopalakrishnan, S., 2016. Guided wave based structural health monitoring: A review. Smart Materials and Structures, 25(5), 053001

Morin, D., 2010. [Online] Available at: http://www.people.fas.harvard.edu/~djmorin/waves/interference.pdf [Accessed 27 Mar. 2016].

Nair, A. and Cai, C.S., 2010. Acoustic emission monitoring of bridges: Review and case studies. Engineering Structures, 32(6), 1704–1714.

Ploss, P., Rupitsch, S.J. and Lerch, R., 2014. Extraction of Spatial Ultrasonic Wave Packet Features by Exploiting a Modified Hough Transform. IEEE Sensors Journal, 14 (7), 2389-2395.

Raghavan, A. & Cesnik, C.E.S., 2007. Review of Guided-wave Structural Health Monitoring. The Shock and Vibration Digest, 39(2), 91–114.

Ren, G.and Jhang, K.Y., 2013. Application of Macrofiber Composite for Smart Transducer of Lamb Wave Inspection. Advances in Materials Science and Engineering, 2013,1–5.

Smart-material.com, 2016. MFC. [Online] Available at http://www.smart-material.com/MFC-product-main.html [Accessed 16 Mar. 2016].

Tiwari, K.A.and Raisutis, R., 2016. Comparative analysis of non-contact ultrasonic methods for defect estimation of composites in remote araes. CBU International Conference Proceedings, 4, 846.

Umchid, S., 2009. Directivity pattern measurement of ultrasound transducers. The International Journal on Applied Biomedical Engineering (IJABME), 2, 39-43.

Voelz, U., 2012. Four-dimensional directivity pattern for fast calculation of the sound field of a phased array transducer. 2012 IEEE International

Wenkang Q. and Wenwu C., 2000. Finite element study on 1-D array transducer design. IEEE Transactions on Ultrasonics, Ferroelectrics and Frequency Control, 47(4), 949–955.

Wilcox, P., 2000. Lamb and SH wave transducer arrays for the inspection of large areas of thick plates. AIP Conference Proceedings.

Wilkie, W.K., Bryant, R.G., High, J.W., Fox, R.L., Hellbaum, R.F., Jalink Jr, A., Little, B.D. and Mirick, P.H., 2000, Low-cost piezocomposite actuator for structural control applications. In SPIE's 7th Annual International Symposium on Smart Structures and Materials: Industrial and Commercial Applications of Smart Structures Technologies, 323-334.

Zagrai, A.N. and Çakan, H., 2010. Magneto-mechanical impedance identification and diagnosis of metallic structures. International Journal of Engineering Science, 48(10), 888–908.

Zhang, K., Han, Z. and Yuan, K., 2013. Long Range Inspection of Rail-Break Using Ultrasonic Guided Wave Excited by Pulse String. Advanced Materials Research, 744, 505-510.